DOI 10.1007/s10891-015-1267-6
Journal of Engineering Physics and Thermophysics, Vol. 88, No. 4, July, 2015

HEAT TRANSFER AND FLOW OF A CASSON FLUID DUE TO A STRETCHING CYLINDER WITH THE SORET AND DUFOUR EFFECTS

A. Mahdy

UDC 536.24

Numerical solutions of the problem on flow and heat transfer of a non-Newtonian fluid outside a stretching permeable cylinder are obtained with regard to suction or blowing and the Soret and Dufour effects. The Casson fluid model is used to characterize the non-Newtonian fluid behavior. The governing partial differential equations are reduced to a system of nonlinear ordinary differential equations by employing similarity transformations, and the obtained equations are solved numerically by using the shooting technique. The main purpose of the study is to investigate the effect of the governing parameters, namely, the Casson, Soret, and Dufour parameters, the suction/injection parameter, and the Prandtl and Reynolds numbers, on the velocity and temperature profiles, as well as on the skin friction coefficient and temperature gradient at the surface.

Keywords*: stretching cylinder, Casson fluid, suction/injection, Soret and Dufour effects.*

Introduction. Transport of heat, mass, and momentum in laminar boundary layers on moving (stretching or inextensible) surfaces is a very important process in many engineering applications. Different aspects of flows over shrinking surfaces have been much investigated. The fluid flow over a stretching cylinder has attracted the interest of many researchers. It should be mentioned that a boundary-layer flow due to a stretching or shrinking surface is a relevant type of flows appearing in many industrial and engineering processes, for example, in polymer and metallurgy industries, such as manufacture and extraction of polymer and rubber sheets, melt spinning, hot rolling, paper production, wire drawing, glass fiber production, etc. In these situations, the quality of the final product depends to a great extent on the rate of cooling in the stretching/shrinking process [1]. Wang [2] investigated a steady flow of an incompressible viscous fluid outside a stretching hollow cylinder in an ambient fluid at rest. This problem was then extended in [3] by including the suction and injection effects. It was reported that injection reduces the skin friction, as well as the heat transfer rate at the surface, while suction acts in the opposite manner. Wang and Ng [4] obtained a similarity solution for the flow due to a stretching cylinder with a partial slip condition at the surface. They found that the slip effect significantly decreases the magnitude of the fluid velocity and shear stress. Wang [5] solved the problem of a natural convection on a vertical stretching cylinder and obtained an exact similarity solution of the Navier–Stokes equations. Ishak, Nazar, and Pop [6] numerically solved the problem of a magnetohydrodynamic flow and heat transfer over a stretching cylinder. They observed that the heat transfer rate at the surface decreases with increase in the value of the magnetic parameter, while the magnitude of the skin friction coefficient increases with this parameter and the Reynolds number.

Furthermore, it has been observed that an energy flux can be generated not only by a temperature gradient, but also by a concentration gradient. The energy flux caused by a concentration gradient is termed the diffusion-thermo (Dufour) effect. On the other hand, a mass flux can be created by a temperature gradient; this is thermodiffusion, i.e., the Soret effect which might become significant when large density differences exist in a flow. Mahdy [7] studied the Soret and Dufour effects in mixed convection of a non-Newtonian fluid in porous media. Srinivas, Muthuraj, and Sakina [8] investigated the influence of heat and mass transfer in a peristaltic flow of a viscous fluid in a vertical asymmetric channel with a slip on the wall. Alam et al. [9] theoretically studied the problem of a steady two-dimensional free convection and mass transfer flow past a continuously moving semi-infinite vertical porous plate in a porous medium, including the Soret and Dufour effects. Bég and Tripathi [10] considered peristaltic pumping with double-diffusive convection in nanofluids. A peristaltic motion with the Soret and Dufour effects was discussed by Hayat, Abbasi, and Obaidat [11]. Mahdy [12] examined the combined effect of spatially stationary surface waves and of the presence of fluid inertia on free convection along a heated

Mathematics Department, Faculty of Science, South Valley University, Qena, Egypt; email: mahdy4@yahoo.com.
Published in Inzhenerno-Fizicheskii Zhurnal, Vol. 88, No. 4, pp. 897–904, July–August, 2015. Original article submitted May 2, 2014; revision submitted December 14, 2014.

 0062-0125/15/8804-0928 ©2015 Springer Science+Business Media New York

vertical wavy surface embedded in a porous medium saturated by an electrically conducting fluid subjected to the diffusion-thermo (Dufour), thermodiffusion (Soret), and magnetic field effects. Adrian [13] numerically investigated the heat and mass transfer characteristics of natural convection about a vertical surface embedded in a saturated porous medium subjected to a magnetic field by taking into account the Dufour and Soret effects. The effect of melting and/or thermodiffusion on convective transport in a non-Darcy porous medium saturated by a non-Newtonian fluid was presented by Kairi and Murthy [14] and Srinivasacharya and RamReddy [15].

On the other hand, interest in the time-independent flow of non-Newtonian fluids with a definite yield value through tubes has grown because of their applications in polymer processing industries. The most popular among these fluids is a Casson one [16]. We can define a Casson fluid as a shear-thinning liquid which is assumed to have an infinite viscosity at zero rate of shear, the yield stress below which no flow occurs, and a zero viscosity at an infinite rate of shear. The Casson model is a well-known rheological model for describing the behavior of non-Newtonian fluids with an yield stress [17]. The model was developed for viscous suspensions of cylindrical particles [18]. Regardless of the types of suspensions, some fluids are particularly well described by this model because of their nonlinear yield-stress-pseudoplastic nature. Examples of such fluids are blood [19], chocolate [20], and xanthan gum solutions [21]. The Casson model fits the flow data better than the more general Herschel–Bulkley model [22, 23] with a power-law dependence for the yield stress [24, 25]. For chocolate and blood, the Casson model is the preferred rheological model. This model seems to fit the nonlinear behavior of yield-stress-pseudoplastic fluids rather well, and its popularity grew since its introduction in 1959. It is relatively simple to use and it is closely related to the Bingham model [24, 25], which is very widely used to describe flows of slurries, suspensions, sludge, and other rheologically complex fluids [26]. Eldabe and Salwa [27] studied a Casson fluid flow between two rotating cylinders. Boyd, Buick, and Green [28] used the Casson fluid model as applied to the steady and oscillatory blood flow. In recent years, a boundary-layer flow of a Casson fluid over bodies of different geometries was considered by many authors. Nadeem, Haq, and Lee [29] investigated an MHD flow of a Casson fluid over an exponentially shrinking sheet. Kumari et al. [30] analyzed peristaltic pumping of an MHD Casson fluid in an inclined channel. Sreenadh, Pallavi, and Satyanarayana [31] studied a Casson fluid flow through an inclined tube of a nonuniform cross section with multiple stenoses. Mukhopadhyay et al. [32] considered an unsteady two-dimensional flow of a non-Newtonian fluid over a stretching surface with a prescribed surface temperature. The details of a steady fully-developed laminar flow of Casson fluids were described in [33]. In view of the non-Newtonian nature of blood in capillaries and filtration/absorption property of the walls, Oka [34] studied blood flow in capillaries with permeable walls, using the Casson fluid model.

Having in mind the above studies on the boundary-layer flow due to a stretching cylinder, we shall investigate two-dimensional flows of a Casson fluid. In addition, the Soret and Dufour effects will be considered together with suction or injection. The Soret effect is connected with the occurrence of a diffusion flux because of a temperature gradient, whereas the Dufour effect, with a heat flux due to a concentration gradient. The fluid flow is induced by a stretching cylinder.

Formulation of the Problem. Let us consider the non-Newtonian Casson fluid steady two-dimensional laminar flow caused by a stretching tube of radius a in the axial direction in a fluid at rest as shown in Fig. 1, where the z axis is directed along the tube axis and the r axis, in the radial direction. It is assumed that the tube surface is kept at a constant temperature T_{w}, the ambient fluid temperature is T_∞, and $T_{\mathrm{w}} > T_\infty$. Viscous dissipation is neglected as it is assumed to be small. The rheological equation of state for an isotropic incompressible flow of a Casson fluid is [27, 35]

$$\tau_{ij} = \begin{cases} 2\left(\mu_B + \dfrac{P_{\mathrm{y}}}{\sqrt{2\pi}}\right) e_{ij}, & \pi > \pi_{\mathrm{c}}, \\ 2\left(\mu_B + \dfrac{P_{\mathrm{y}}}{\sqrt{2\pi_{\mathrm{c}}}}\right) e_{ij}, & \pi < \pi_{\mathrm{c}}, \end{cases}$$

where $\tau_{ij} = e_{ij}e_{ij}$, π is the product of the components of the deformation rate tensor with itself, and π_{c} is a critical value of this product based on the non-Newtonian model. If a shear stress smaller than the yield stress is applied to the fluid, the latter behaves like a solid, whereas if the shear stress is greater than the yield stress, it starts to move. Considering the balance laws of mass, linear momentum, and energy, with the help of the Boussinesq approximation for the body force term in the momentum equation we can write the equations governing this flow in the form

$$\frac{\partial(rw)}{\partial z} + \frac{\partial(ru)}{\partial r} = 0\,, \tag{1}$$

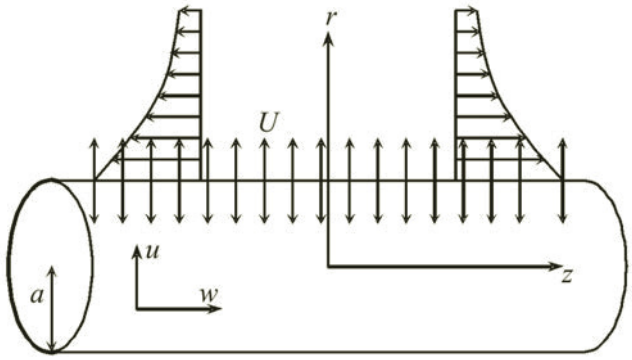

Fig. 1. Schematic model of the problem.

$$w\frac{\partial w}{\partial z}+u\frac{\partial w}{\partial r}=\nu\left(1+\frac{1}{\beta}\right)\left(\frac{\partial^2 w}{\partial r^2}+\frac{1}{r}\frac{\partial w}{\partial r}\right), \tag{2}$$

$$w\frac{\partial u}{\partial z}+u\frac{\partial u}{\partial r}=-\frac{1}{\rho}\frac{\partial P}{\partial r}+\nu\left(1+\frac{1}{\beta}\right)\left(\frac{\partial^2 u}{\partial r^2}+\frac{1}{r}\frac{\partial u}{\partial r}-\frac{u}{r^2}\right), \tag{3}$$

$$w\frac{\partial T}{\partial z}+u\frac{\partial T}{\partial r}=\alpha\left(\frac{\partial^2 T}{\partial r^2}+\frac{1}{r}\frac{\partial T}{\partial r}\right)+\frac{Dk}{c_p c_s}\left(\frac{\partial^2 C}{\partial r^2}+\frac{1}{r}\frac{\partial C}{\partial r}\right), \tag{4}$$

$$w\frac{\partial C}{\partial z}+u\frac{\partial C}{\partial r}=D\left(\frac{\partial^2 C}{\partial r^2}+\frac{1}{r}\frac{\partial C}{\partial r}\right)+\frac{Dk}{T_{\mathrm{m}}}\left(\frac{\partial^2 T}{\partial r^2}+\frac{1}{r}\frac{\partial T}{\partial r}\right). \tag{5}$$

The corresponding boundary conditions are

$$r=a\colon\ u=U=-ba\gamma\ ,\quad w=w_{\mathrm{w}}=2bz\ ,\quad T=T_{\mathrm{w}}\ ,\quad C=C_{\mathrm{w}}\ ;$$
$$r\to\infty\colon\ w\to 0\ ,\quad T\to T_{\infty}\ ,\quad C\to C_{\infty}\ . \tag{6}$$

Here b is a positive constant. It should be noted that γ is constant with $\gamma > 0$ and $\gamma < 0$ corresponding to mass suction and mass injection (blowing), respectively. In order to get a similarity solution of the problem, we introduce the following nondimensional variables:

$$\eta=\frac{r^2}{a^2}\ ,\quad w=2bf'(\eta)z\ ,\quad u=-\frac{ba}{\sqrt{\eta}}f(\eta)\ ,$$
$$\theta(\eta)=\frac{T-T_{\infty}}{T_{\mathrm{w}}-T_{\infty}}\ ,\quad \phi(\eta)=\frac{C-C_{\infty}}{C_{\mathrm{w}}-C_{\infty}}\ . \tag{7}$$

Substituting Eq. (7) into Eqs. (2), (4), and (5), we obtain the following ordinary differential equations, which are locally similar:

$$\frac{1+\beta}{\beta}\left(\eta\frac{d^3 f}{d\eta^3}+\frac{d^2 f}{d\eta^2}\right)+\mathrm{Re}\left(f\frac{d^2 f}{d\eta^2}-\left(\frac{df}{d\eta}\right)^2\right)=0\ , \tag{8}$$

$$\eta\frac{d^2\theta}{d\eta^2}+\frac{d\theta}{d\eta}+\mathrm{Pr}\,\mathrm{Re}\,f\frac{d\theta}{d\eta}+\mathrm{Pr}\,\mathrm{Df}\left(\eta\frac{d^2\phi}{d\eta^2}+\frac{d\phi}{d\eta}\right)=0\ , \tag{9}$$

$$\eta \frac{d^2\phi}{d\eta^2} + \frac{d\phi}{d\eta} + \mathrm{Sc}\,\mathrm{Re}\, f \frac{d\phi}{d\eta} + \mathrm{Sc}\,\mathrm{Sr}\left(\eta \frac{d^2\theta}{d\eta^2} + \frac{d\theta}{d\eta}\right) = 0 . \tag{10}$$

The Prandtl, Reynolds, and Schmidt numbers, as well as the Soret and Dufour parameters, are defined as

$$\mathrm{Pr} = \frac{\nu}{\alpha}, \quad \mathrm{Re} = \frac{ba^2}{2\nu}, \quad \mathrm{Sc} = \frac{\nu}{D}, \quad \mathrm{Sr} = \frac{Dk(T_\mathrm{w} - T_\infty)}{T_\mathrm{m}\nu(C_\mathrm{w} - C_\infty)}, \quad \mathrm{Df} = \frac{Dk(C_\mathrm{w} - C_\infty)}{c_p c_\mathrm{s}\nu(T_\mathrm{w} - T_\infty)} .$$

The boundary conditions (6) turn into

$$f(1) = \gamma, \quad f'(1) = \theta(1) = \phi(1) = 1, \quad f'(\infty) \to 0, \quad \theta(\infty) \to 0, \quad \phi(\infty) \to 0, \tag{11}$$

where the prime denotes ordinary differentiation with respect to the similarity variable.

The exact solution of Eq. (8) at Re = 1 is given as

$$f(\eta) = \sqrt{1 + \frac{1}{\beta}}\left(1 - \exp\left(-\frac{\eta}{\sqrt{1 + \frac{1}{\beta}}}\right)\right).$$

The pressure can be determined by integrating Eq. (3) in the form

$$\frac{P - P_\infty}{\rho b \nu} = -\left(\frac{\mathrm{Re}}{\eta} f^2 + 2\left(1 + \frac{1}{\beta}\right) f'\right). \tag{12}$$

Results and Discussion. The boundary-layer flow and heat and mass transfer of a non-Newtonian Casson fluid occurring due to a stretching cylinder in the presence of the Soret and Dufour effects, as well as suction/injection ones, are considered. The set of coupled equations (8)–(10) is highly nonlinear and cannot be solved analytically. Together with boundary conditions (11), they form a two-point boundary-value problem which can be solved by using the routine bvpc45 in MATLAB by converting it into an initial value problem. In this case we choose a finite value of η corresponding to $\eta \to \infty$, say η_f. Care has been taken in choosing η_f for a given set of parameters because a fixed value of η_f for all calculations may lead to inaccurate results. The obtained results account for the roles of several nondimensional parameters, namely, the Reynolds number, Casson parameter, Prandtl number, Schmidt number, and the Soret and Dufour parameters. The case where the Casson parameter is zero has been also considered, and the results were compared with the previously published results. Tables 1 and 2 present the numerical values of the skin friction coefficient ($-f''(1)$) and the temperature gradient ($-\theta'(1)$) along with the results reported in [2, 3], and excellent agreement is seen.

Figure 2 illustrates the effect of the Casson parameter β on the nondimensional velocity (f'), temperature (θ), concentration (ϕ), and the stream function (f) distributions for a steady case with mass suction and injection. The increasing values of the Casson parameter, i.e., the decreasing values of the yield stress (the fluid behaves as a Newtonian one as the Casson parameter becomes large), suppress the velocity. An increase in β reduces the transport rate, so that the boundary-layer thickness decreases. It is observed that $f'(\eta)$ and the associated boundary-layer thickness are decreasing functions of β. An increase in β leads to increasing temperature and concentration for a steady motion (Fig. 2b and c). Thickening of the thermal boundary layer occurs due to the increase in the elasticity stress parameter. It can also be seen from Fig. 2a that the momentum boundary-layer thickness decreases as β increases, which induces an increase in the absolute value of the velocity gradient at the surface.

Figure 3 shows the influence of the Soret and Dufour parameters on the temperature and concentration distributions. It is seen that as the Soret parameter increases and the Dufour parameter decreases, both the temperature and concentration decrease. Moreover, an increase in Sr tends to decrease the absolute value of $\theta'(1)$ and to increase $\phi'(1)$.

The velocity distribution for various values of the Reynolds number is given in Fig. 4, and the velocity, temperature, and concentration gradient distributions at the tube surface, in Fig. 5. It is worth mentioning that the Reynolds number characterizes the relative significance of the inertia effect compared to the viscous one. It is observed that both the stream

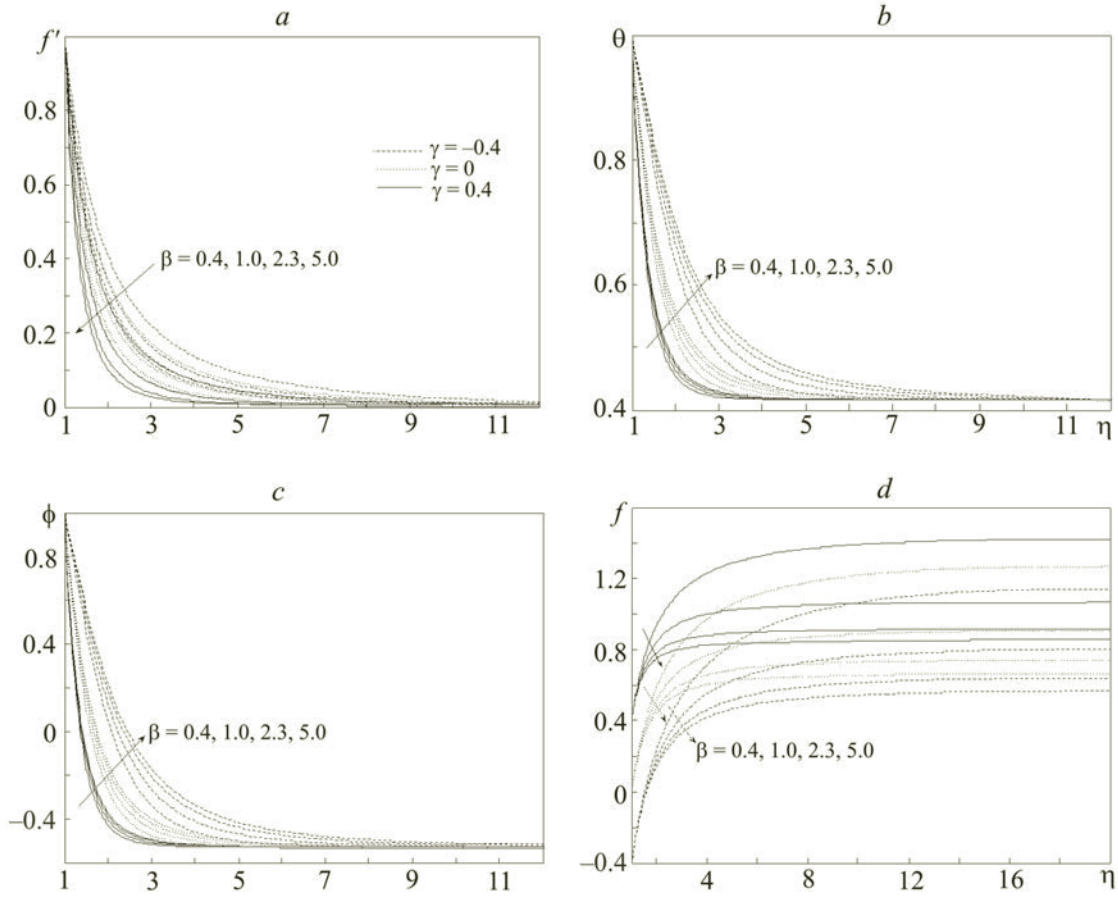

Fig. 2. Velocity (a), temperature (b), concentration (c), and stream function (d) distributions at Sr = 1.2, Re = 5, Pr = 7, Df = 0.36, and Sc = 1.6 for various values of the Casson parameter.

TABLE 1. Values of $-f''(1)$ for Various Reynolds Numbers

Re	γ = 0			γ = –0.5		γ = 0.5	
	[2]	[3]	Present	[3]	Present	[3]	Present
0.5	0.88220	0.8827	0.88691	0.7719	0.77555	1.0084	1.01309
1.0	1.17776	1.1781	1.17953	0.9623	0.96339	1.4400	1.44160
2.0	1.59390	1.5941	1.59434	1.1810	1.18115	2.1468	2.1471
5.0	2.41745	2.4175	2.4175	1.4811	1.48111	3.9308	3.93088
10.0	3.34445	3.3445	3.34447	1.6776	1.67756	6.6222	6.62227

TABLE 2. Values of $-\theta'(1)$ for Various Prandtl Numbers

Pr	γ = 0			γ = –0.5		γ = 0.5	
	[2]	[3]	Present	[3]	Present	[3]	Present
0.7	1.568	1.5683	1.56878	0.2573	0.25823	4.1961	4.19617
2.0	3.035	3.0360	3.03596	0.063	0.06315	11.1517	11.15149
7.0	6.160	6.1592	6.15813	0	0	36.6120	36.61141
10.0	10.77	7.4668	7.46477	0	0	51.7048	51.70485

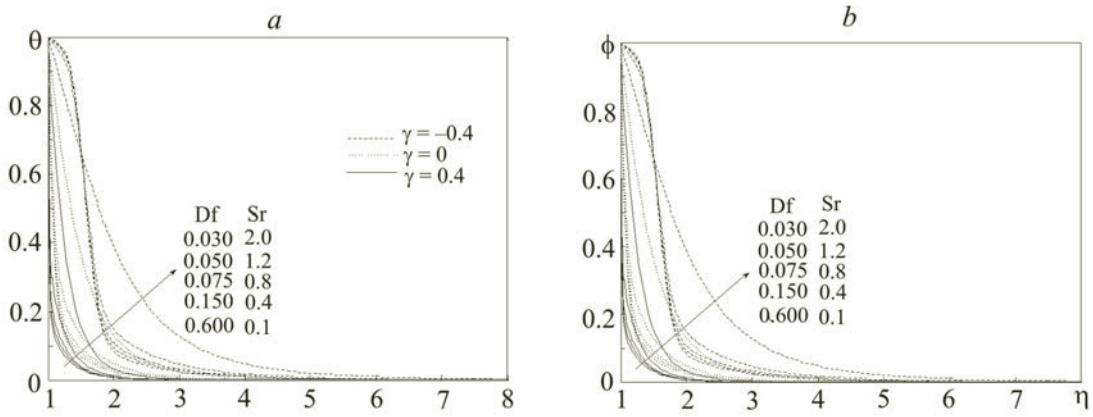

Fig. 3. Temperature (a) and concentration (b) distributions at β = 1.8, Re = 5, Pr = 7, and Sc = 1.6 for various values of the Dufour and Soret parameters.

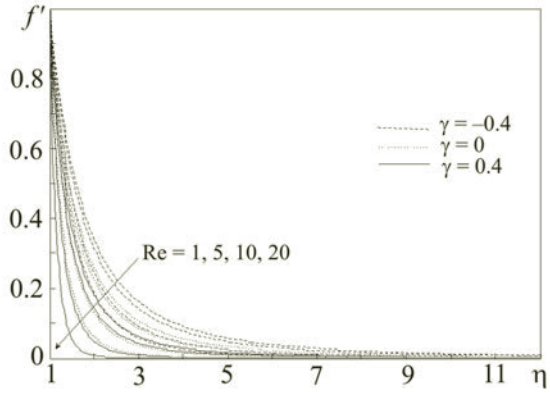

Fig. 4. Velocity distribution at Sr = 1.2, β = 1.8, Pr = 7, Df = 0.36, and Sc =1.6 for various values of the Reynolds number.

function and velocity decrease as the Reynolds number increases. The velocity approaches zero at some large distance from the tube surface. It is seen from Fig. 4 that the velocity boundary-layer thickness decreases as Re increases, which implies an increasing velocity gradient, i.e., an increasing magnitude of the skin friction coefficient (Table 1). The same behavior can be observed for the temperature and concentration gradients that increase with Re (Figs. 5b and c).

The Prandtl number is the ratio of the momentum diffusivity to thermal diffusivity. It is shown that the temperature and thermal boundary-layer thickness decrease with increasing Pr. The temperature gradient at the tube surface is negative for all values of Pr, as seen from numerical results, which means that heat is always transferred from the tube surface to the ambient fluid. Fluids with lower Prandtl numbers possess higher thermal conductivities (and thicker thermal boundary layers), so that in this situation heat can diffuse from the tube surface faster than in fluids with higher Pr (and thinner boundary layers).

The Schmidt number is an important parameter in heat and mass transfer processes as it characterizes the ratio of the thicknesses of the viscous and concentration boundary layers. The effect of the Schmidt number on the species concentration is similar to the Prandtl number effect on the temperature. That is, an increase in the value of Sc significantly decreases the species concentration and boundary-layer thickness with a slight increase in the fluid temperature. This decrease in the solute concentration causes a reduction in the solutal buoyancy effect, resulting in a lesser induced flow along the tube surface. The effect of the Soret number on the heat and mass transfer rate at the tube surface is illustrated by Fig. 6. It is seen that the heat transfer rate decreases, while the mass transfer rate increases, with increasing Soret number. It is also shown that the heat transfer rate increases with the Dufour number.

In addition, Figs. 2–6 show the role of the suction/blowing parameter γ. With increase in this parameter, the fluid velocity, temperature, and concentration are found to decrease. The decrease in the fluid velocity in the boundary layer in

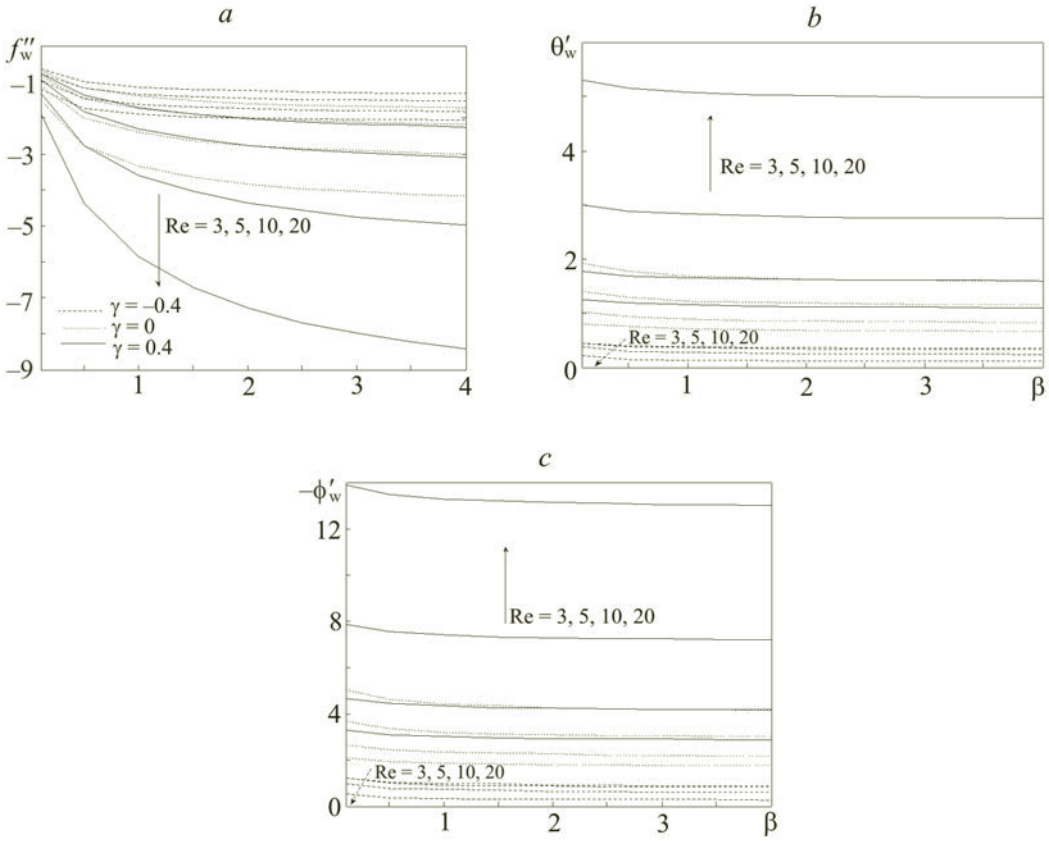

Fig. 5. Velocity (a), temperature (b), and concentration (c) gradients vs. the Casson parameter at Sr = 1.2, Pr = 7, Df = 0.36, and Sc = 1.6 for various values of the Reynolds number.

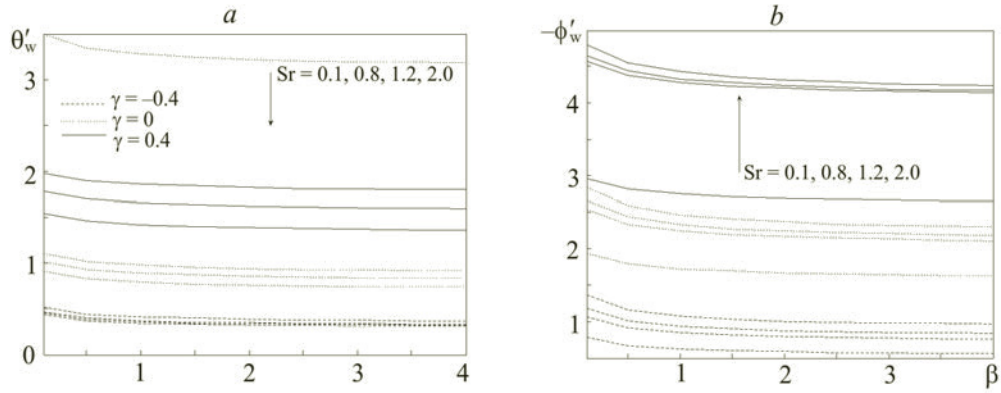

Fig. 6. Temperature (a) and concentration (b) gradients vs. the Casson parameter at Re = 5, Pr = 7, Df = 0.36, and Sc = 1.6 for various values of the Soret parameter.

turn decreases the wall shear stress. An increase in γ causes thinning of the boundary layer. However, the temperature and concentration are found to decrease with increasing γ. This causes a decrease in the heat and mass transfer rate.

Conclusions. A steady two-dimensional flow of a non-Newtonian Casson fluid occurring due to a stretching cylindrical tube has been investigated. Similarity solutions were obtained for a linearly stretching tube with a constant surface temperature. The effects of the Reynolds, Prandtl, and Schmidt numbers and of the Casson, Soret, and Dufour parameters on the flow and heat transfer characteristics were examined. It is shown that an increase in the value of the Casson parameter β suppresses the velocity, whereas the temperature increases with β. As the Soret parameter increases and the Dufour parameter decreases, both the temperature and concentration decrease.

NOTATION

a, radius of a cylinder; b, positive constant; C, concentration; c_p, specific heat at constant pressure; c_s, concentration susceptibility; D, mass diffusivity; Df, Dufour parameter; e_{ij}, component of the deformation rate rensor; f, nondimensional stream function; k, thermal diffusion ratio; P, pressure; P_y, component of the yield stress tensor; Pr, Prandtl number; Re, Reynolds number; Sc, Schmidt number; Sr, Soret parameter; T, temperature; u, w, velocity components; U, velocity of a stretching tube; z, r, coordinates; α, thermal diffusivity; β, Casson parameter; γ, suction or injection parameter; η, similarity variable; θ, nondimensional temperature; μ_B, plastic dynamic viscosity of a non-Newtonian fluid; ν, kinematic viscosity; ρ, density; τ_{ij}, component of the stress tensor; ϕ, nondimensional concentration; ψ, stream function. Indices: f, finite; m, mean; w, conditions at the cylinder surface; ∞, conditions in the free stream.

REFERENCES

1. N. Bachok, A. Ishak, and I. Pop, Boundary layer stagnation-point flow and heat transfer over an exponentially stretching/shrinking sheet in a nanofluid, *Int. J. Heat Mass Transf.*, **55**, 8122–8128 (2012).
2. C. Y. Wang, Fluid flow due to a stretching cylinder, *Phys. Fluids*, **31**, 466–468 (1988).
3. A. Ishak, R. Nazar, and I. Pop, Uniform suction/blowing effect on flow and heat transfer due to a stretching cylinder, *Appl. Math. Model*., **32**, 2059–2066 (2008).
4. C. Y. Wang and C. Ng, Slip flow due to a stretching cylinder, *Int. J. Non-Linear Mech*., **46**, 1191–1194 (2011).
5. C. Y. Wang, Natural convection on a vertical stretching cylinder, *Commun. Nonlinear Sci. Numer. Simul*., **17**, 1098–1103 (2012).
6. A. Ishak, R. Nazar, and I. Pop, Magnetohydrodynamic (MHD) flow and heat transfer due to a stretching cylinder, *Energy Convers. Manage*., **49**, 3265–3269 (2008).
7. A. Mahdy, Soret and Dufour effect on double diffusion mixed convection from a vertical surface in a porous medium saturated with a non-Newtonian fluid, *J. Non-Newtonian Fluid Mech*., **165**, 568–575 (2010).
8. S. Srinivas, R. Muthuraj, and J. Sakina, A note on the influence of heat and mass transfer on a peristaltic flow of a viscous fluid in a vertical asymmetric channel with wall slip, *Chem. Ind. Chem. Eng. Quart*., **18**, 483–493 (2012).
9. M. S. Alam, M. Ferdows, M. Ota, and M. A. Maleque, Dufour and Soret effects on steady free convection and mass transfer flow past a semi-infinite vertical porous plate in a porous medium, *Int. J. Appl. Mech. Eng.*, **11**, 535–545 (2006).
10. O. Bég and D. Tripathi, Mathematical simulation of peristaltic pumping with double diffusive convection in nanofluids: a bio-nano-engineering model, *J. Nanoeng. Nanosyst*., **225**, 99–114 (2012).
11. T. Hayat, F. M. Abbasi and S. Obaidat, Peristaltic motion with Soret and Dufour effects, *Magnetohydrodynamics*, **47**, 295–302 (2011).
12. A. Mahdy, MHD non-Darcian free convection from a vertical wavy surface embedded in porous media in the presence of Soret and Dufour effect, *Int. Commun. Heat Mass Transf*., **36**, 1067–1074 (2009).
13. P. Adrian, Influence of a magnetic field on heat and mass transfer by natural convection from vertical surfaces in porous media considering Soret and Dufour effects, *Int. J. Heat Mass Transf*., **47**, 1467–1472 (2004).
14. R. R. Kairi and P. V. S. N. Murthy, The effect of melting and thermo-diffusion on natural convection heat mass transfer in a non-Newtonian fluid saturated non-Darcy porous medium, *Open Transp. Phenom. J*., **1**, 7–14 (2009).
15. D. Srinivasacharya and Ch. RamReddy, Mixed convection heat and mass transfer in a non-Darcy micropolar fluid with Soret and Dufour effects, *Nonlinear Anal. Model. Control*, **16**, 100–115 (2011).
16. N. Casson, in: C. C. Mills, Ed., *Rheology of Disperse Systems*, Pergamon, New York (1959), Ch. 5.
17. E. O. Reher, D. Haroske, and K. Kohler, Strömungen nicht-Newtonscher Flüssigkeiten, *Chem. Technol*., **21**, No. 3, 137–143 (1969).
18. W. P. Walwander, T. Y. Chen, and D. F. Cala, An approximate Casson fluid model for tube flow of blood, *Biorheology*, **12**, 111–119 (1975).
19. G. Cokelet, H. Shin, A. Britten, and R. E. Wells, Rheology of human blood — measurement near and at zero shear rate, *Trans. Soc. Rheol*., **7**, 303–317 (1963).
20. J. Chevalley, An adaptation of the Casson equation for the rheology of chocolate, *J. Texture Stud*., **22**, 219–229 (1991).
21. F. Garcia-Ochoa and J. A. Casas, Apparent yield stress in xanthan gum solutions at low concentrations, *Chem. Eng. J*., **53**, B41–B46 (1994).

22. E. A. Kirsanov and S. V. Remizov, Application of the Casson model to thixotropic waxy crude oil, *Rheol. Acta*, **38**, 172–176 (1999).
23. D. D. Joye, Application of yield stress-pseudoplastic fluid models to pipeline transport of sludge, in: *Proc. 30th Mid-Atlantic Industrial Waste Conf. on Hazardous and Industrial Wastes*, Technomic Publ. Corp., Lancaster, PA/Basel, 1998, pp. 567–575.
24. R. B. Bird, W. E. Stewart, and E. N. Lightfoot, *Transport Phenomena*, Wiley, New York (1960).
25. W. L. Wilkinson, *Non-Newtonian Fluids*, Pergamon, New York (1960).
26. S. W. Churchill, *Viscous Flows: The Practical Use of Theory*, Butterworths, Boston (1988), Ch. 5.
27. N. T. M. Eldabe and M. G. E. Salwa, Heat transfer of MHD non-Newtonian Casson fluid flow between two rotating cylinders, *J. Phys. Soc. Jpn*., **64**, 41–64 (1995).
28. J. Boyd, J. M. Buick, and S. Green, Analysis of the Casson and Carreau–Yasuda non-Newtonian blood models in steady and oscillatory flow using the lattice Boltzmann method, *Phys. Fluids*, **19**, 93–103 (2007).
29. S. Nadeem, R. U. Haq, and C. Lee, MHD flow of a Casson fluid over an exponentially shrinking sheet, *Scientia Iranica*, **19**, 1550–1553 (2012).
30. P. K. Kumari, M. V. Murthy, M. Reddy, and Y. V. K. Kumar, Peristaltic pumping of a magnetohydrodynamic Casson fluid in an inclined channel, *Adv. Appl. Sci. Res*., **2**, 428–436 (2011).
31. S. Sreenadh, A. R. Pallavi, and Bh. Satyanarayana, Flow of a Casson fluid through an inclined tube of non-uniform cross section with multiple stenoses, *Adv. Appl. Sci. Res*., **2**, No. 5, 340–349 (2011).
32. Swati Mukhopadhyay, Prativa Ranjan De, Krishnendu Bhattacharyya, and G. C. Layek, Casson fluid flow over an unsteady stretching surface, *Ain Shams Eng. J.*, **4**, 933–938 (2013).
33. Y. C. Fung, *Biomechanics: Mechanical Properties of Living Tissues*, Springer-Verlag, New York (1981), Ch. 3.
34. S. Oka, Non-Newtonian blood flow in a capillary with a permeable wall, in: *Proc. Festschrift of Harold Wayland Symposium*, California Inst. of Tech., Pasadena (1979).
35. E. M. A. Elbashbeshy and M. A. A. Bazid, Heat transfer over an unsteady stretching surface, *Heat Mass Transf*., **41**, 1–4 (2004).